Shear-Induced Rearrangement of Self-Assembled PEG-Lipids Structures in Water

S. Rangelov,*,†,‡ M. Almgren,† Ch. Tsvetanov,‡ and K. Edwards†

Department of Physical Chemistry, University of Uppsala, Box 532, 751 21 Uppsala, Sweden, and Institute of Polymers, Bulgarian Academy of Sciences, 1113 Sofia, Bulgaria

Received February 28, 2002; Revised Manuscript Received June 12, 2002

ABSTRACT: A number of nonionic PEG-lipids were synthesized via anionic polymerization of ethylene oxide using 1,3-didodecyloxypropan-2-ol as a starting material. The two aliphatic chains as well as the PEG moieties are linked to the glycerol skeleton via ether linkages. By varying the ethylene oxide polymerization time, PEG moieties of degrees of polymerization ranging from 30 to 92 were constructed. The PEG-lipids were characterized by ^{1}H nuclear magnetic resonance and gel permeation chromatography. In aqueous solution they formed spontaneously micellar and possibly lamellar aggregates. The latter were seen in the relaxation time distribution spectra as low-amplitude diffusive slow modes. The particles responsible for the slow mode behavior were eliminated by centrifugation, and light scattering in an extended temperature interval was carried out. At elevated temperatures particles with increasing density were formed. The solutions were found to be sensitive to shear forces as revealed by comparing the relaxation time distribution spectra of vigorously stirred, filtered, or extruded solutions with those of the starting solutions. Objects identified as bilayer structures were found in the extruded solutions. They were visualized by cryogenic transmission electron microscopy. The micellization regions were investigated by a fluorescence probing technique.

Introduction

Lipid vesicles, liposomes, have the potential to function as drug delivery carriers since their amphiphatic structure and compositions are well fitted to solubilize and encapsulate both hydrophobic and hydrophilic active substances. The colloidal stability of the liposomes, however, is limited: their survival time in the bloodstream is short, and they are quickly taken up by macrophages. In the past decade, however, vesicle compositions which give prolonged vesicle circulation time in the bloodstream have been discovered,[1−7] and the interest for liposomes as potent drug delivery carriers has been reborn.

The enhanced longevity of liposomes is achieved by incorporation of polymer-derivatized phospholipids into the lipid bilayers. Poly(ethylene glycol) (PEG) is the most extensively used polymer for this purpose. There is general consensus that the PEG chains grafted onto the bilayer act as a steric repulsive barrier around the liposome and prevent the various blood proteins from interacting with the membrane.

PEG-derivatized phospholipids referred to as PEG-lipids are nowadays commercially available in a variety of molecular weights of the PEG chain and a diversity of lipid anchors—1,2-distearoylphosphatidylethanolamine, 1,2-dipalmitoylphosphatidylethanolamine, 1-palmitoyl-2-oleylphosphatidylethanolamine, etc. The PEG chain is covalently attached to the lipid anchor most commonly via a carbamate linkage. The latter is known to introduce a net negative charge at the membrane surface which in turn may change the properties of the membrane substantially.[8,9] In addition, the replacement of an ester bond by an ether bond was found to change the dipole potential.[10,11] Consequently, the synthesis and utilization of PEG-lipids with alkyl chains and a PEG-moiety linked to the glycerol skeleton via ether linkages provide opportunities to modify the properties of the sterically stabilized liposomes.

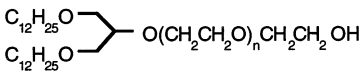

Figure 1. Chemical structure of the PEG-lipids. n = 30, 44, 52, and 92.

In a previous paper the synthesis, characterization, and polymerization ability of a novel epoxide monomer were described.[12] The monomer contains a polymerizable epoxy group that is linked to a glycerol skeleton bearing two aliphatic groups connected via ether linkages (aliphatic double chain). A number of copolymers with ethylene oxide (EO) were prepared, and their self-assembly and ability to stabilize liposomes are under investigation.[13,14] These copolymers contain short blocks of repeating units bearing an aliphatic double chain. For comparison, a number of PEG-lipids bearing only one lipid anchor of the same structure were also prepared. The present work deals with the synthesis and investigation of the behavior of the above PEG-lipids in aqueous solution. The chemical structure is presented in Figure 1. The hydrophobic moiety of these artificial lipids consists of two fully saturated C_{12} aliphatic chains attached to a glycerol skeleton via ether linkages. This moiety mimics the hydrophobic anchor of the naturally occurring constituents of the cell membranes, the phospholipids. PEG chains of various degrees of polymerization are also attached to the lipid anchors via ether linkages. The aqueous solution properties of the PEG-lipids are studied by light scattering, fluorescence, and cryogenic transmission electron microscopy.

Experimental Section

Materials. All solvents and reagents were supplied by Fluka or Aldrich. Ethylene oxide was purchased from Neochim AD, Bulgaria. The starting alcohol, 1,3-didodecyloxypropan-

† University of Uppsala.
‡ Bulgarian Academy of Sciences.

10.1021/ma020313+ CCC: $22.00
Published on Web 08/03/2002

2-ol (DDP), was prepared according to a procedure described elsewhere.[12] The solvents were purified by standard methods whereas the reagents were used as received. The solutions of each PEG-lipid were prepared by dissolving the appropriate amount of PEG-lipid in purified water taken from Millipore Super-Q-System.

Synthesis of PEG-Lipids. 0.709 g (1.66×10^{-3} mol) of DDP and 0.056 g (1.0×10^{-3} mol) of KOH were placed in a 50 mL three-necked flask fitted with nitrogen and EO inlets and a reflux condenser. The mixture was heated and at 110 °C was purged with EO for 60 min. After that the residue was cooled to room temperature and dissolved in methylene chloride. The polymer was isolated by precipitation in hexane and washed with portions of 30 mL hexane until no more hexane-soluble fraction was extracted. 3.42 g of a white solid was isolated and dried in a vacuum up to a constant weight.

The syntheses of the other PEG-lipids were carried out as described above. The purity of the products was checked by thin-layer chromatography using silica gel plates (Riedel-de Haen Silica gel 60 F 254) and a methanol:water 5:1 solvent system. The plates were developed using iodine vapor.

Methods. *Nuclear Magnetic Resonance (NMR).* ^{1}H NMR spectra were recorded at 250 MHz on a Bruker 250 spectrometer. The samples were prepared as solutions in $CDCl_3$. The chemical shifts are given in ppm from tetramethylsilane. All spectra were recorded at 25 °C.

Gel Permeation Chromatography (GPC). The GPC system (Waters) consisted of four styragel columns with nominal pore sizes of 100, 500, 500, and 1000 Å, eluted with tetrahydrofuran at 40 °C. The flow rate of the eluent was 1 mL/min. Samples were prepared as solutions in tetrahydrofuran. Elution volumes were referenced to toluene as internal standard. Calibration was done with PEG standards, and derived weight-average molar masses and degrees of polymerization were determined as if samples were PEG.

Fluorescent Measurements. Fluorescence spectra, with the fluorescent probe pyrene, were recorded on a SPEX-fluorolog 1650 0.22 m double spectrometer (SPEX Industries Inc., Edison, NJ). The emission measurements were performed between 350 and 450 nm with an excitation wavelength at 320 nm. Slit widths were set to 1 mm, and the temperature was controlled by means of a water-jacketed cuvette holder connected to a thermostat.

Appropriate volumes of a stock solution of pyrene in ethanol were transferred into a number of cylindrical vials. The solvent was removed under a stream of nitrogen and thereafter under vacuum for 24 h. Proper amounts of centrifuged PEG-lipid stock solutions and purified water (Millipore Super-Q-System) were added to the vials to give a final volume of 2 mL and a final pyrene concentration of 5×10^{-7} M. The samples were incubated in the dark for 24 h at room temperature.

Light Scattering (LS). The LS setup consists, as described previously,[15] of a 488 nm Ar ion laser and the detector optics with an ITT FW 130 photomultiplier and ALV-PM-PD amplifier−discriminator connected to an ALV-5000 autocorrelator built into a computer. The cylindrical scattering cells were sealed and then immersed in a large-diameter thermostated bath containing the index matching fluid decalin. Measurements were made at different angles in the range 50−130° and at different concentrations and temperatures. Information on the molecular weight and the second virial coefficient was obtained from the dependence of the reduced scattered intensity Kc/R_Θ on the concentration (c) and the scattering angle (Θ) measured in the simultaneous static and dynamic experiments. Here $K = (4\pi^2 n^2/N_A\lambda^4)(dn/dc)^2$, N_A is Avogadro's constant, and λ is the wavelength. The refractive index increment (dn/dc) was measured in a differential refractometer with Rayleigh optics. For the present systems, dn/dc varied within the PEG-lipid composition, and the values were between 0.128 and 0.137 mL g^{-1} at the wavelength used and 25 °C. The Rayleigh ratio was determined as $R_\Theta = [(I - I_0)/I_{ref}]R_{ref}(n/n_{ref})^2$. Here $n = 1.33$ is the solvent refractive index and n_{ref} that of toluene. I is the measured total time-average scattered intensity, I_0 that of the solvent, water, and I_{ref} that of toluene. Toluene was used as the reference scatterer ($R_{ref} = 4.0 \times 10^{-3}$ m^{-1} at $\lambda = 488$ nm[15]).

Analysis of the dynamic data was performed by fitting the experimentally measured $g_2(t)$, the normalized intensity autocorrelation function, which is related to the electrical field correlation function $g_1(t)$ by the Siegert relationship:[16]

$$g_2(t) - 1 = \beta|g_1(t)|^2 \tag{1}$$

where β is a factor accounting for deviation from ideal correlation. For polydisperse samples, $g_1(t)$ can be written as the inverse Laplace transform (ILT) of the relaxation time distribution, $\tau A(\tau)$:

$$g_1(t) = \int \tau A(\tau) \exp(-t/\tau)\, d \ln \tau \tag{2}$$

where t is the lag time. The relaxation time distribution, $\tau A(\tau)$, is obtained by performing ILT using the constrained regularization algorithm REPES,[17] which minimizes the sum of the squared differences between the experimental and calculated $g_2(t)$. A mean diffusion coefficient D is calculated from the second moment of each peak as $D = \Gamma/q^2$, where q is the magnitude of the scattering vector $q = (4\pi n/\lambda)\sin(\Theta/2)$ and $\Gamma = 1/\tau$ is the relaxation rate of each mode. Here Θ is the scattering angle, n the refractive index of the medium, and λ the wavelength of the light in a vacuum.

Within the dilute regime, D varies linearly with the concentration according to

$$D = D_0(1 + k_D C + ...) \tag{3}$$

where D_0 is the diffusion coefficient at infinite dilution and k_D is the hydrodynamic "virial" coefficient related to the second virial coefficient A_2 by

$$k_D = 2A_2M - k_f - 2\nu_2 \tag{4}$$

Here M is the molar mass, k_f defines the concentration dependence of the friction coefficient in $f = f_0(1 + k_f C + ...)$, and ν_2 is the partial specific volume.

The Stokes−Einstein equation relates D_0 to the hydrodynamic radius (R_h):

$$R_h = kT/(6\pi\eta D_0) \tag{5}$$

kT is the thermal energy factor, and η is the temperature-dependent viscosity of the solvent.

Cryogenic Transmission Electron Microscopy (Cryo-TEM). Transmission electron microscopy observations were conducted on a Zeiss EM 902 A instrument operating at 80 kV. The procedure for the sample preparation is described in the following. A drop of the solution is deposited on an electron microscopy copper grid coated by a perforated polymer film. The excess of the liquid is blotted by a filter paper, leaving a thin film of the solution on the grid. The above operations are performed in a special chamber where the environmental conditions (constant temperature and high humidity) are under strict control. The film on the grid is vitrified by plunging the grid into liquid ethane. The vitrified sample is then transferred to the microscope for observation. The observation and the transfer are done at temperatures below 108 K in order to prevent the formation of ice crystal.

Results and Discussion

PEG-Lipid Synthesis. The PEG-lipids were prepared by anionic polymerization of EO in the presence of a base starting at the hydroxyl group of DDP. By varying the time of polymerization, PEG moieties of different molecular weights were obtained. The average molecular weights and the corresponding degrees of polymerization of the PEG moieties were determined

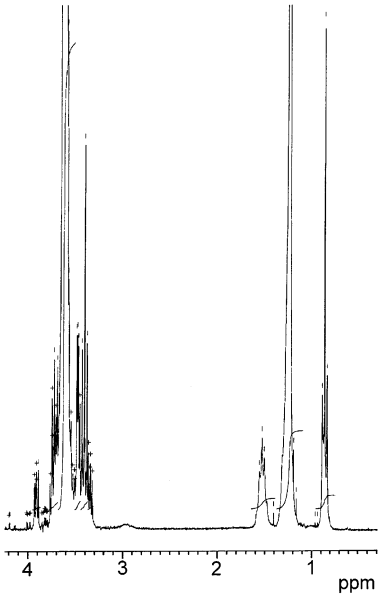

Figure 2. ^{1}H NMR spectrum of DDP(EO)$_{52}$.

Table 1. Polymerization Time, Molecular Weight Distribution, Nominal Molecular Weights, and Average Compositions of the PEG-Lipids

polymerization time (min)	mol wt distribution (GPC)	nominal mol wt (NMR)	composition
30	1.20	1747	DDP(EO)$_{30}$
60	1.19	2363	DDP(EO)$_{44}$
90	1.15	2715	DDP(EO)$_{52}$
120	1.13	4475	DDP(EO)$_{92}$

from the ^{1}H NMR spectra from the relative intensities of the resonances of the methylene protons of the PEG moieties at 3.5−3.7 ppm and the methyl protons of the dodecyl chains at 0.8 ppm.[12] A ^{1}H NMR spectrum of DDP(EO)$_{52}$ is shown in Figure 2. The polymerization time, the molecular weight distribution, the nominal molecular weight, and the average compositions of the investigated PEG-lipids are given in Table 1.

Aqueous Solution Properties. Dynamic light scattering (DLS) experiments were performed on solutions of PEG-lipids in the concentration range (0.5−10.0) × 10^{-3} g/mL at 25 °C. The distributions were invariably bimodal containing a low-intensity slow mode together with a dominant peak with an amplitude that varied within the samples and concentrations and accounted for about 90% of the intensity at an angle 90° (Figure 3a). The dominant modes of the different PEG-lipids corresponded to aggregates of hydrodynamic radii of 50−70 Å, whereas the slow modes corresponded to hydrodynamic radii of hundreds of nanometers. The presence of a slow mode in pure PEG-lipid/water systems as well as spontaneous formation of both micellar and/or lamellar phases has been reported earlier by a number of research groups.[18−24] It has been also found that the nonmicellar aggregates can be dissolved by the addition of salts or by heating and incubation for several hours at elevated temperatures.[24] Neither of these procedures, however, were found to be effective in our case. The fact that the increase of temperature had no effect ruled out the possibility of existence of nonmicellar aggregates in a L_β phase that melt only at higher temperatures. Indeed, DSC thermograms for the pure PEG-lipids are similar to those of related copolymers published elsewhere,[12] showing two well-separated endothermic peaks (thermograms not presented). The high-temperature peak corresponds to the melting of the PEG moiety, whereas the low-temperature peak (0−2 °C) is attributed to the melting of the aliphatic double chain residue. Consequently, no material in a gel phase is expected to be present at 25 °C.

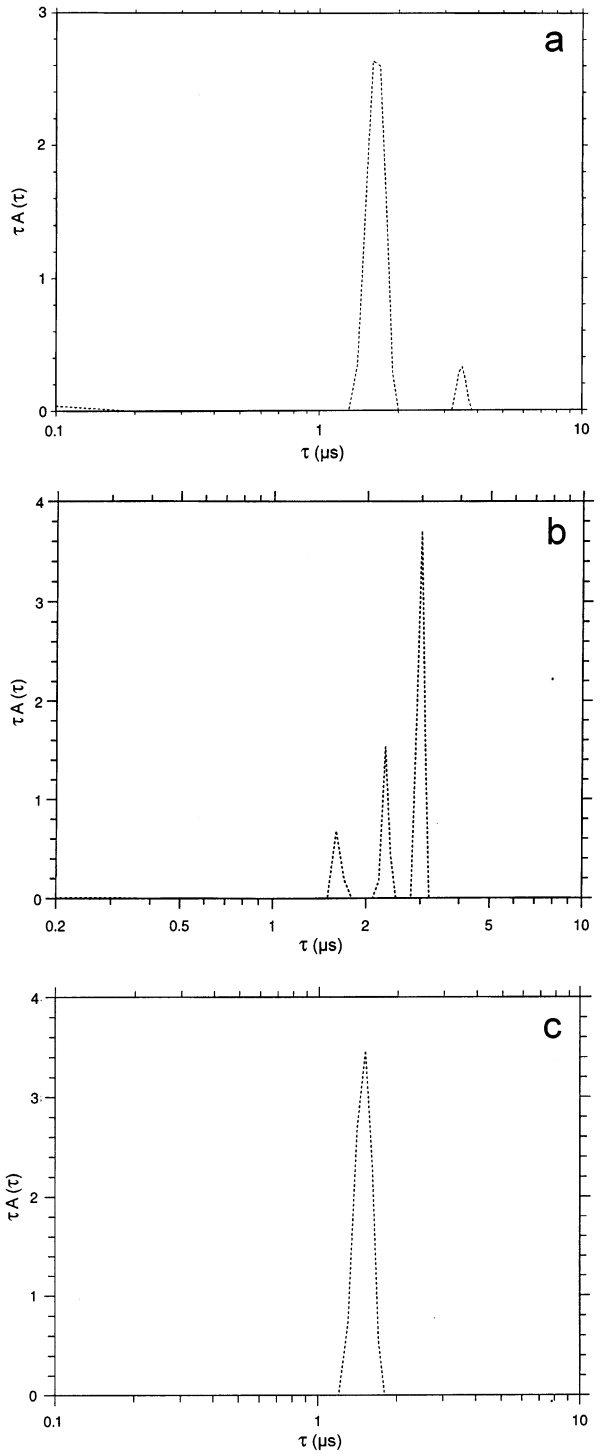

Figure 3. Relaxation time distributions measured at an angle 90° and temperature 25 °C of (a) the original 1.0 × 10^{-3} g/mL DDP(EO)$_{30}$ solution. (b) The solution in (a) after extrusion through 100 nm pore size filter. (c) The solution in (a) after centrifugation at 13 000 rpm for 40 min.

If the slow mode behavior of our PEG-lipids was a result of the presence of impurities, although the polymers were adequately purified and only one spot was observed by thin-layer chromatography, the impu-

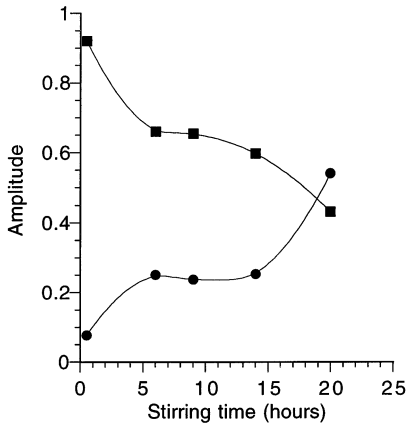

Figure 4. Variations of the amplitudes of the fast (squares) and slow (circles) modes of 1.0×10^{-3} g/mL $DDP(EO)_{44}$ at angle 90° and temperature 25 °C as a function of the stirring time.

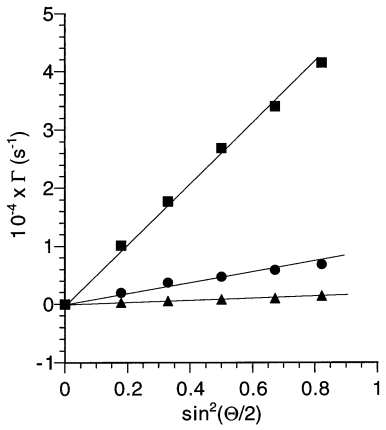

Figure 5. Relaxation rates (Γ) of the fast (squares), intermediate (circles), and slow (triangles) modes as a function of $\sin^2(\Theta/2)$ for an extruded $DDP(EO)_{30}$ solution. The lines through the data points represent linear fits to the data.

rities would be easily removed by filtration through small pore size filters. It turned out, however, that the filtration had an opposite effect: the aggregates responsible for the slow mode behavior were not removed, but on the contrary, their contribution to the scattered light intensity increased, suggesting that a shear-induced rearrangement took place. Moreover, even the stirring time was found to affect the relaxation time distribution as shown in Figure 4, where the amplitudes of the fast and slow modes of a 1.0×10^{-3} g/mL solution of $DDP(EO)_{44}$ are given as a function of the stirring time.

Shear-Induced Rearrangement. To test the assumption of shear-induced transition, solutions of 1.0×10^{-3} g/mL concentration were extruded 30 times through 100 nm pore size filters. This procedure is known to yield vesicles of synthetic and natural lipids in water.[25−27] Typical distributions of relaxation times before and after the extrusion are shown in Figure 3a,b. As seen, there was little change in the position of the fast peak, i.e., the one dominant before the extrusion. In contrast, the slow modes became faster, and usually another slow mode appeared. All peaks were shown to be diffusive from the linear plots of the relaxation rates vs $\sin^2 \Theta/2$ (Figure 5). The diffusion coefficients were determined from the slopes of the linear fit. The intermediate and slow modes corresponded to particles of hydrodynamic radii of several tens to hundreds of nanometers, respectively.

Cryo-TEM was employed to visualize the aggregates obtained after the extrusion. It should be emphasized, however, that although the amplitudes of the slow modes are usually higher than those of the fast modes, the weight concentration of these particles is still low. Therefore, the micrographs in Figure 6 are dominated by spherical micelles observed as small black dots in the background. Anyway, objects unambiguously identified as bilayer structures were clearly seen in all micrographs. These are closed liposome structures of spherical (arrows A in Figure 6a), elongated (arrows B in Figure 6a,b), and irregular (arrow E in Figure 6c and the object in Figure 6d) shapes. Note the abundance of vesicles of irregular shape in Figure 6c and the presence of cylindrical micelles (arrows F in Figure 6c).

Although the extrusion methods are widely used to produce unilamellar and relatively monodisperse liposomes,[25−27] little attention has been paid to the detailed mechanism of this process or to the role of for example the physical properties of the lipid dispersions in the shear-induced transition. Not only extrusion, but shearing in general can have strong influence on the structure of aqueous solutions of amphiphilic molecules: alignment and breakup of lamellae as well as transitions from a lamellar to a vesicle phase under the influence of shear have been reported.[28−35] Therefore, the shear sensitivity of our systems was not a surprise. Although the detailed mechanism is far from clear, we will outline a rough model of the shear-induced phase transition. In the original noncentrifuged dispersions the micellar phase coexists with a small fraction of large aggregates of lamellar structure. During the extrusion the latter block part of the pores of the filter and when forced into the pores and exposed to the high shear they break up into smaller particles. This is seen in the spectra of the relaxation time distribution as "fastening" of the slow modes (Figure 3a,b). During the flow through the pores the micelles and the lamellar flakes get in intimate contacts, facilitating interactions and exchange of molecules between the two types of structures. The increasing amplitude of the slow modes after the extrusion (Figure 3b) implies a net transfer of molecules from the micelles to the lamellar flakes or vesicles.

Micellization Region. The association behavior of the PEG-lipids was investigated by a pyrene solubilization technique. Pyrene has been widely used as a polarity probe because of its unique photophysical properties. Its vibronic fluorescence spectrum exhibits five peaks, and the ratio of the intensities of the first to the third peaks (I/III) is known to be sensitive to the polarity of the environment.[36] The observed magnitude of I/III depends somewhat on the apparatus and the experimental setup; values in the range 1.6−1.9 have been reported in water and 0.6-0.9 in nonpolar solvents. The variation of I/III with the concentration of $DDP(EO)_{92}$ is presented in Figure 7. At very low PEG-lipid concentrations the I/III ratio is high—1.58−1.60; i.e., pyrene experiences an aqueous environment. (A value of 1.62 was obtained for pyrene in pure water.) When the PEG-lipid concentration increases, a decrease of I/III was observed, revealing the presence or formation of hydrophobic domains. At high polymer concentrations a low plateau with I/III value of ca. 1.06 is reached, indicating that all pyrene is in the hydrophobic environment. In contrast to conventional surfactants, where I/III decreases over a rather narrow concentration range, here the I/III vs *C* curve shows a sigmoidal shape,

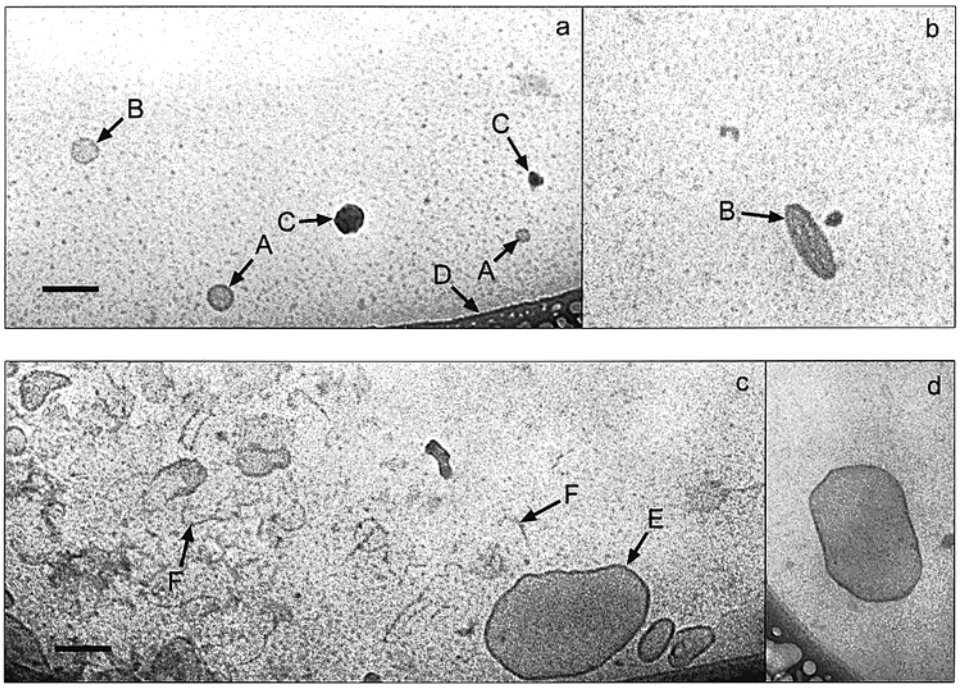

Figure 6. Cryo-TEM micrographs of extruded 1.0×10^{-3} g/mL solutions of $DDP(EO)_{44}$ (a) and (b) and of $DDP(EO)_{92}$ (c) and (d). Arrows A, B, and E denote closed liposome strucutres. Cylindrical micelles are indicated with arrows F. Arrows C and D denote ice crystals deposited on the sample surface after vitrification and the edge of the polymer film, respectively. Bar = 100 nm applies also for (b) and (d).

Table 2. Fluorescence Characterization Data of the PEG-Lipids in the Temperature Interval 25−45 °C[a]

polymer	T (°C)	C_o	C_p	C_p/C_o	I/III (low plateau)
$DDP(EO)_{30}$	25	2.8×10^{-7}	5.0×10^{-5}	179	0.96
	35	4.2×10^{-8}	2.7×10^{-5}	643	0.94
	45	2.8×10^{-8}	2.7×10^{-5}	964	0.95
$DDP(EO)_{44}$	25	1.1×10^{-6}	4.6×10^{-5}	42	1.06
	35	4.6×10^{-7}	4.6×10^{-5}	100	1.06
	45	3.4×10^{-7}	4.6×10^{-5}	135	1.04
$DDP(EO)_{52}$	25	1.8×10^{-6}	5.0×10^{-5}	28	1.07
	35	1.8×10^{-6}	6.0×10^{-5}	33	1.01
	45	9.0×10^{-7}	5.5×10^{-5}	61	0.99
$DDP(EO)_{92}$	25	2.2×10^{-6}	5.0×10^{-5}	23	1.07
	35	1.1×10^{-6}	5.0×10^{-5}	45	1.07
	45	5.5×10^{-7}	5.0×10^{-5}	91	1.04
$(didodecyl)_2PEG20K$	25	1.7×10^{-7}	2.2×10^{-5}	131	0.86

[a] C_o and C_p are the concentrations in M at which I/III starts to decrease and stabilizes at its lowest value, respectively; C_p/C_o is a measure of the broadness of the transition region; and I/III (low plateau) gives the values of I/III at the low plateau.

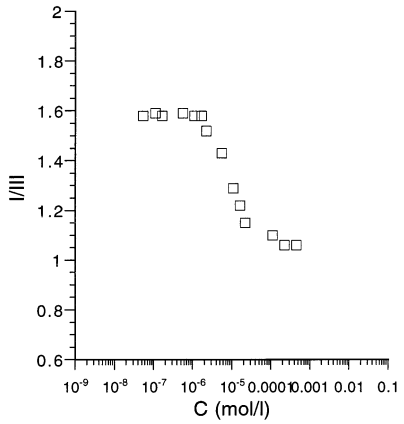

Figure 7. Variation of the intensity ratio I/III of the fluorescence spectrum of pyrene in aqueous solutions of $DDP(EO)_{92}$ at 25 °C.

and the transition is much more gradual. Because of the broadness of the transition region, it is not clear where the critical micellization concentration (cmc) is located. A number of parameters, the concentration at the onset of the I/III decrease (C_o), the concentration at the low plateau (C_p), the values of I/III at the low plateau, and the ratio C_p/C_o as a measure of the broadness of the transition region, were extracted from the data and collected in Table 2. The results obtained at elevated temperatures and for $(didodecyl)_2PEG20K$, aliphatic double chain end-capped PEG 20000,[13,37] were included as well.

As seen from Figure 7 and Table 2 the transition regions are broad. The more gradual decrease of I/III compared to the sharp and sudden change of the conventional surfactants shows a less cooperative aggregation process.[38] The transition broadens with decreasing hydrophilicity of the species, reaching C_p/C_o ratio of 179 for $DDP(EO)_{30}$ at 25 °C. The behavior of the most hydrophilic polymer, however, $(didodecyl)_2$-PEG20K, contradicts the observed trend: its transition is very broad with C_p/C_o of 130. In this case the broadening of the transition interval can be attributed to intramolecular aggregation of the end lipid-mimetic

anchors. Thus, ring-shaped molecules with hydrophobic domains big enough to solubilize pyrene may form even at high dilution, which causes the broadening of the transition. The assumption that ring-shaped molecules are formed is corroborated by the results from DLS, showing appearance of a fast mode together with the aggregate mode upon the dilution of the $(didodecyl)_2$-PEG20K micellar solutions. The fast mode was attributed to unassociated ring-shaped molecules.[13] Besides the hydrophobicity of $DDP(EO)_{30}$, the relatively broad molecular weight distribution of this polymer may contribute to the broadening of the transition. The broad distribution combined with the low molecular weight means that a fraction of polymer chains with very low degree of ethoxylation is present. These molecules are more hydrophobic than the rest and consequently prone to aggregation at very low concentrations. With increasing degree of ethoxylation and decreasing molecular weight distribution (Table 1), the fraction of such hydrophobic molecules progressively decreases and makes the transition sharper.

An interesting measure is also the concentrations at which the low I/III values plateau is reached, i.e., the concentrations at which the micellization process is considered to be completed. This concentration depends only slightly on molecular weight and temperature (Table 2). In contrast, the onset of the aggregation is shifted toward the low concentrations with decreasing hydrophilicity of the samples. With increasing temperature the data become more scattered, which makes it difficult to precisely determine the onset of the I/III decrease. Anyway, a trend to shift the onset toward low concentrations was observed, indicating that hydrophobic microdomains start to form at lower concentrations at elevated temperatures.

As noted above, the magnitude of I/III depends on the fraction of pyrene present in the nonpolar environment and on the polarity of this environment. When the ratio I/III stabilizes at its lowest values, i.e., the low plateau is reached, it is assumed that all pyrene is solubilized in the aggregates. However, there are still differences in the I/III values of the PEG-lipids. It is still unclear why the values of I/III differ since the hydrophobic anchors that build up the cores of the micelles are the same, and consequently the polarity of the environment is expected to be the same. It is tempting to relate this to the aggregation numbers of the particles[39,40] (see the next section), although the I/III values for $DDP(EO)_{44}$ and $DDP(EO)_{52}$ are somewhat erratic.

Micellar Size, Molecular Weight, and Aggregation Number. It was possible to remove the particles responsible for the slow mode behavior by centrifugation as evidenced by the relaxation time distribution of a 1.0×10^{-3} g/mL solution of $DDP(EO)_{30}$ before and after the centrifugation (Figure 3a,c). As seen only a single population of particles was found after the centrifugation. The diffusion coefficients, D, were determined from the slopes of the linear fit of the data plotted as relaxation rates vs $\sin^2(\Theta/2)$ (Figure 8a). Then the values of D at various concentrations were plotted against the particle concentration (Figure 8b), and using the Stokes−Einstein equation, the hydrodynamic radii were calculated. They are given in the last column of Table 3.

Static light scattering (SLS) experiments were carried out on centrifuged solutions in the same concentration range as DLS. The measurements were done at a single

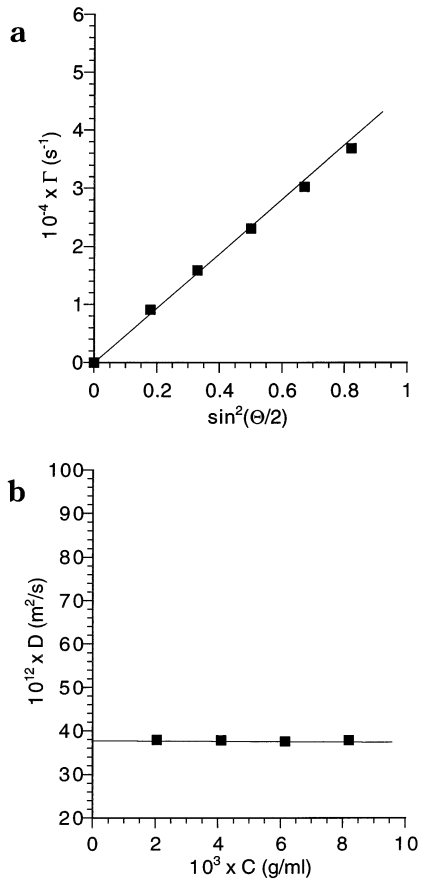

Figure 8. (a) Relaxation rate (Γ) as a function of $\sin^2(\Theta/2)$ for centrifuged 8.184×10^{-3} g/mL solution of $DDP(EO)_{52}$. (b) Concentration dependence of the diffusion coefficient for $DDP(EO)_{52}$. The lines through the data points represent linear fits to the data.

Table 3. Static and Dynamic Light Scattering Characterization Data of Nonionic PEG-Lipid Micelles in Water at 25 °C

PEG-lipid	$10^{-3}M_w$ (g/mol)	10^4A_2 (mol mL/g^2)	N_{agg}	R_h (Å)
$DDP(EO)_{30}$	128.4	3.42	73	52.1
$DDP(EO)_{44}$	185.8	2.55	79	62.7
$DDP(EO)_{52}$	148.5	1.93	55	66.5
$DDP(EO)_{92}$	108.7	3.36	24	65.0

angle, $\Theta = 90°$, since no angular dependence of the scattered light intensity was found. The apparent weight-average molecular weights and the second virial coefficients were determined from the dependence of $Kc/R_{\Theta=90}$ vs the PEG-lipid concentration (Figure 9). It should be emphasized here that the weight concentration of the particles responsible for the slow mode, i.e., the amount of material removed by centrifugation, is negligible: with ratios of the diffusion coefficients D_f/D_s of approximately 10 (here f and s denote the fast and slow mode, respectively) and relative amplitudes $A_s/A_f = 0.12$, and using the approach given by Alami et al.,[41] the relative weight concentrations C_s/C_f was calculated to be about 6.6×10^{-2}. Anyway, the concentrations were recalculated, and the SLS data thus obtained are collected in Table 3. The weight-average molecular weight values are in agreement with those of commercial PEG-lipids.[24] The second virial coefficients are positive, indicating favorable aggregate/solvent interactions. The aggregation numbers, N_{agg}, were estimated using the nominal molecular weights

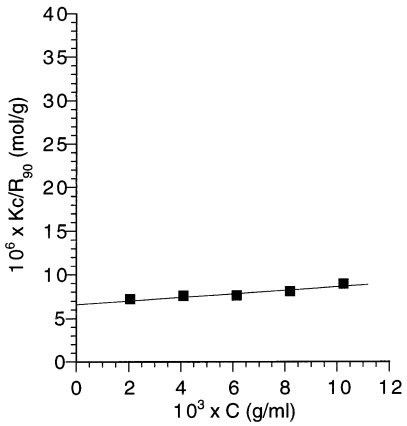

Figure 9. Reduced scattering intensity, Kc/R_{90}, as a function of the concentration for $DDP(EO)_{52}$. The line through the data points represents the linear fit to the data.

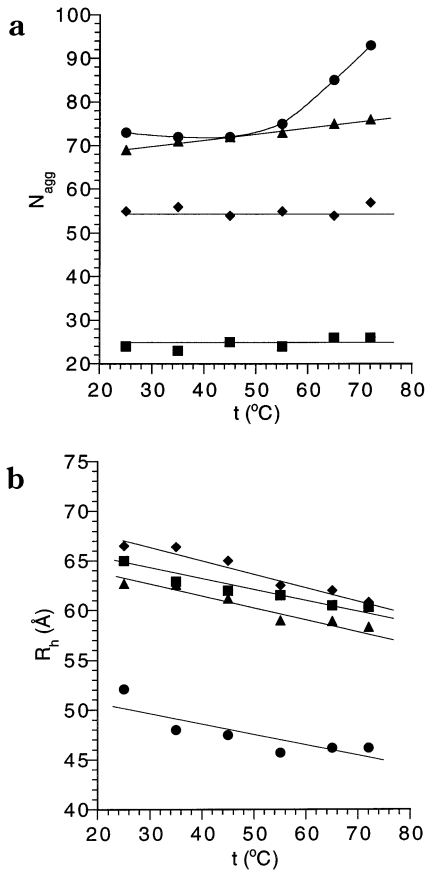

Figure 10. Temperature dependence of the aggregation numbers (a) and hydrodynamic radii (b) for $DDP(EO)_{30}$ (circles), $DDP(EO)_{44}$ (triangles), $DDP(EO)_{52}$ (diamonds), and $DDP(EO)_{92}$ (squares). The lines and curves through the data points are drawn to guide the eye.

of the species. Generally, N_{agg} increased with decreasing hydrophilicity of the PEG-lipid.

Effect of Temperature. The behavior of the PEG-lipids was examined at elevated temperatures. LS experiments were carried out on centrifuged solutions in the concentration range $(2.0-10.0) \times 10^{-3}$ g/mL. The distributions were invariably monomodal in the whole temperature interval studied (25−72 °C). LS data expressed as values of N_{agg} and R_h are given in Figure 10. As seen, N_{agg} practically did not change with the temperature for the hydrophilic members of the series $DDP(EO)_{92}$ and $DDP(EO)_{52}$, whereas for the hydrophobic ones, $DDP(EO)_{30}$ and $DDP(EO)_{44}$, it was found to increase (Figure 10a). The increase was slight for the latter and considerable for the former PEG-lipid. In contrast, R_h was seen to decrease weakly with increasing temperature (Figure 10b). This finding is somewhat surprising and contraintuitive but can be explained in terms of formation of more compact and denser particles with increasing temperature. In our previous paper,[13] the formation of PEG domains in the aggregate cores and the dehydration of the PEG chains leading to shrinking of the cores and a decrease of the corona thickness were suggested to result in a decrease of the hydrodynamic radii of particles obtained from copolymers bearing short blocks of repeating lipid-mimetic anchors in a selective solvent at elevated temperatures. In the present case the formation of PEG domains in the cores is unlikely: the size of the micelles is too small and close to the theoretical one estimated assuming a spherical shape of the particles and using literature data for the volumes of the component groups[42] and experimental data for the aggregation numbers. Moreover, R_h typically decreases by 6−7% in contrast to the hydrodynamic radii of the above-mentioned copolymers which were found to decrease by 15−20%.[13] Therefore, similarly to the micelles of ethylene oxide−propylene oxide block copolymers, Pluronics, the changes of the size of the particles are considered to be related mainly to the solvation of the PEG corona.[43,44]

Conclusions

The association behavior of a series of nonionic PEG-lipids in water was studied by fluorescence probing, dynamic and static light scattering, and cryogenic transmission electron microscopy. The main conclusions of the present study are summarized in the following.

The results from fluorescence indicate that the association process is less cooperative than for the conventional surfactants. It can be concluded that the broadness of the concentration interval at which the micellization occurs is dependent on the hydrophilicity of the polymer and its molecular weight distribution, i.e., the less hydrophilic the polymer and the higher the polydispersity, the broader the transition interval. Upon a temperature increase, the formation of hydrophobic domains shifts to lower polymer concentrations which subsequently causes broadening of the transition region.

The weight-average molecular weights, the second virial coefficients, the diffusion coefficients, and the hydrodynamic radii of the micelles were determined by dynamic and static light scattering. Micelles of weight-average molecular weights up to 185.8×10^3 g/mol are formed, which corresponds to aggregation numbers of 24−79. The latter were found to increase with decreasing hydrophilicity of the PEG-lipids.

At elevated temperatures more compact and denser particles are formed: with an increase of temperature the hydrodynamic radii of the micelles decrease progressively, whereas the micellar aggregation numbers remain practically unchanged for the hydrophilic members of the series or increase for the hydrophobic ones. This trend is most pronounced for the most hydrophobic member, $DDP(EO)_{30}$.

The solutions were found to be shear sensitive. The shear-induced changes were studied by means of DLS and cryo-TEM. The results show that the application of shear leads to formation of slow diffusive particles identified as bilayer structures. A rough model of the shear-induced rearrangement is proposed.

Acknowledgment. We thank G. Karlsson for helping us with the electron microscopy studies and W. Brown for stimulating discussions. N. Bergstrand is thanked for her assistance with the fluorescence measurements. The synthetic part of the study was supported by the Bulgarian National Fund "Scientific Research" (project X-808). Financial support from the Swedish Technical Research Council is gratefully acknowledged.

References and Notes

(1) Needham, D.; Hristova, K.; McIntosh, T.; Dewhirst, M.; Wu, N.; Lasic, D. *J Liposome Res.* **1992**, *2*, 411.
(2) Williams, S.; Alosco, T.; Mayhew, E.; Lasic, D.; Blankert, R. *Cancer Res.* **1993**, *53*, 3964.
(3) Uster, P. S.; Allen, T. M.; Daniel, B. E.; Mendez, C. J.; Newman, M. S.; Zhu, G. Z. *FEBS Lett.* **1996**, *386*, 243.
(4) Allen, T. M. *Curr. Opin. Colloid Interface Sci.* **1996**, *1*, 645.
(5) Johnsson, M.; Bergstrand, N.; Edwards, K. *J. Liposome Res.* **1999**, *9*, 53.
(6) Allen, T. M.; Hansen, C. B.; Lopes-de-Menezes, D. E. *Adv. Drug Delivery Rev.* **1995**, *16*, 267.
(7) Woodle, M. *Adv. Drug Delivery Rev.* **1995**, *16*, 249.
(8) Silvander, M.; Johnsson, M.; Edwards, K. *Chem. Phys. Lipids* **1998**, *97*, 15.
(9) Flewelling, R. F.; Hubbell, W. L. *Biophys. J.* **1986**, *49*, 531.
(10) Franklin, J. C.; Cafiso, D. S. *Biophys. J.* **1993**, *65*, 289.
(11) Gawrisch, K.; Ruston, D.; Zimmerberg, J.; Parsegian, V. A.; Rand, R. P.; Fuller, N. *Biophys. J.* **1992**, *61*, 1213.
(12) Rangelov, S.; Petrova, E.; Berlinova, I.; Tsvetanov, Ch. *Polymer* **2001**, *42*, 4483.
(13) Rangelov, S.; Almgren, M.; Tsvetanov, Ch.; Edwards, K. *Macromolecules* **2002**, *35*, 4770.
(14) Rangelov, S.; Edwards, K.; Almgren, M.; Karlsson, G. *Langmuir*, submitted.
(15) Rangelov, S.; Brown, W. *Polymer* **2000**, *41*, 4825.
(16) Chu, B. *Laser Light Scattering, 2*; Academic Press: New York, 1991.
(17) Jakes, J. *Czech. J. Phys. B* **1988**, *38*, 1305.
(18) Morone, N.; Ueda, T.; Okumura, Y.; Rosilio, V.; Haratake, M.; Higashi, N.; Zheng, Z.; Sunamoto, J. *Polym. Prepr.* **1998**, *39*, 172.
(19) Kenworthy, A. K.; Simon, S. A.; McIntosh, T. J. *Biophys. J.* **1995**, *68*, 1903.
(20) Edwards, K.; Johnsson, M.; Karlsson, G.; Silvander, M. *Biophys. J.* **1997**, *73*, 258.
(21) Lasic, D. D.; Woodle, M. C.; Martin, F. J.; Valentincic, T. *Period. Biol.* **1991**, *93*, 287.
(22) Blume, G.; Cevc, G. *Biochim. Biophys. Acta* **1993**, *1146*, 157.
(23) Koynova, R.; Tenchov, B.; Rapp, G. *Colloids Surf. A* **1999**, *149*, 571.
(24) Johnsson, M.; Hansson, P.; Edwards, K. *J. Phys. Chem. B* **2001**, *105*, 8420.
(25) Fendler, J. *Membrane Mimetic Chemistry*; Wiley: New York, 1982.
(26) Hope, M. J.; Bally, M. B.; Webb, G.; Cullis, P. R. *Biochim. Biophys. Acta* **1985**, *812*, 55.
(27) New, R. R. C. In *Liposomes as Tools in Basic Research and Industry*; Philippot, J. R., Schuber, F., Eds.; CRC Press: Boca Raton, FL, 1995.
(28) Mang, J. T.; Kumar, S.; Hammouda, B. *Europhys. Lett.* **1994**, *28*, 489.
(29) Penfold, J.; Staples, E.; Khan Lodhi, A.; Tucker, I.; Tiddy, G. J. T. *J. Phys. Chem. B* **1997**, *101*, 66.
(30) Ctes, M.; Milner, S. F. *Phys. Rev. Lett.* **1989**, *62*, 1865.
(31) Diat, O.; Roux, D.; Nallet, F. *J. Phys. II* **1993**, *3*, 1427.
(32) Diat, O.; Roux, D.; Nallet, F. *Phys. Rev. E* **1995**, *51*, 3296.
(33) Berghausen, J.; Zipfel, J.; Lindner, P.; Richtering, W. *Europhys. Lett.* **1998**, *43*, 683.
(34) Bergmeier, M.; Gradzielski, M.; Hoffmann, H.; Mortensen, K. *J. Phys. Chem. B* **1999**, *103*, 1605.
(35) Escalante, J. I.; Gradzielski, M.; Hoffmann, H.; Mortensen, K. *Langmuir* **2000**, *16*, 8653.
(36) Kalyanasundaram, K.; Thomas, J. K. *J. Am. Chem. Soc.* **1977**, *99*, 2039.
(37) Rangelov, S.; Tsvetanov, Ch. *Polym. Bull. (Berlin)* **2001**, *46*, 471.
(38) Alami, E.; Almgren, M.; Brown, W. *Macromolecules* **1996**, *29*, 5026.
(39) Almgren, M.; Grieser, F.; Thomas, J. K. *J. Am. Chem. Soc.* **1979**, *101*, 279.
(40) Hansson, P.; Almgren, M. *J. Phys. Chem. B* **2000**, *104*, 1137.
(41) Alami, E.; Almgren, M.; Brown, W.; Francois, J. *Macromolecules* **1996**, *29*, 2229.
(42) Nagle, J. F.; Tristram-Nagle, S. *Biochim. Biophys. Acta* **2000**, *1469*, 159.
(43) Almgren, M.; Brown, W.; Hvidt, S. *Colloid Polym. Sci.* **1995**, *273*, 2.
(44) Yang, L.; Alexandridis, P.; Steytler, D.; Kositza, M.; Holzwarth, J. *Langmuir* **2000**, *16*, 8555.

MA020313+